MECSOL 2022 - Proceedings of the 8th International Symposium on Solid Mechanics
M.L. Bittencourt, J. Labaki, L.C.M. Vieira Jr. and E. Mesquita (Editors), Campinas SP, Brazil, October 17th to 19th, 2022

Numerical multi-scale analysis of elastic-plastic porous media using the direct FE^2 method

Tiago dos Santos[1] and Rodrigo Rossi[2]

[1] Departamento de Engenharia Mecânica, Universidade Federal de Santa Maria, Av. Roraima, 1000, Prédio 7, Santa Maria, RS, Brazil
[2] Departamento de Engenharia Mecânica, Universidade Federal do Rio Grande do Sul, Rua Sarmento Leite, 425, Porto Alegre, RS, Brazil

Abstract. This work evaluates the mechanical behaviour of elastic-plastic porous materials with cylindrical voids using a direct FE^2 multi-scale framework. The study investigates the influence of the void volume fraction on the overall structural behaviour considering a simple tensile test of a plate. Despite its simplicity, the numerical study allows comparing the direct FE^2 method with direct numerical simulations, in which the material heterogeneities are modelled considering a single scale. The comparison allows assessing specific numerical aspects related to the direct FE^2 framework, such as its accuracy and the corresponding computational cost. This is a first step of our group toward multi-scale analysis employing the direct FE^2 to model the mechanical behaviour of heterogeneous materials considering more complex morphology and loading conditions.
Keywords: Porous materials, Elastic-plastic materials, Multi-scale analysis, Direct FE^2 method

INTRODUCTION

It is a matter of fact that heterogeneous materials are ubiquitous in nature and in industrial activities. The heterogeneous features are increasingly being used in an effort to design new multifunctional composite materials aiming at provide more efficient and sustainable alternatives to, e.g., aerospace, transportation, electronics, and medical industries (see e.g. Matouš et al. (2017)). In this scenario, suitable constitutive models are mandatory in order to understand and to predict the corresponding material behaviour, thus guiding the development, the design and the application of new composites. Understanding the behaviour of complex media is not an easy task, since their overall properties will depend on the underlying microstructures which may have different morphology, volume fraction, and properties of the constituents (Steinmann & Javili, 2016). Given the complex microstructural behaviour of engineered materials, the prediction of the overall response of composite materials requires appropriate methods. In this regard, the computational multi-scale analysis has proved to be a high-fidelity modelling alternative to precisely describe the coupled behaviour of heterogeneous materials, thus accelerating the discovery, the development and the virtual testing of new composites. In this sense, we can cite the pioneer works of Feyel & Chaboche (2001), Kouznetsova et al. (2001) and Yuan & Fish (2008), to mention a few. See also the reviews due to Steinmann & Javili (2016), Matouš et al. (2017) and recently Raju et al. (2021). Most of the computational multi-scale approaches employ the finite element analysis at both the macroscopic and the microscopic scales, which are solved concurrently, thus giving to rise to FE^2 methods. Although traditional FE^2 approaches can model the behaviour of heterogeneous materials with high-accuracy, it is well-known that such approaches are very time consuming and require sophisticated computational tools to carry the simulations out. Aiming at reducing the computational cost, alternative techniques have been proposed to perform multi-scale computational analysis. Recently, Tan et al. (2020) proposed a direct two scale finite element (direct FE^2) framework to deal with multi-scale problems. The direct FE^2 method can reduce the computational cost in comparison with the conventional FE^2 setup. In addition, it can be implemented within commercial finite element codes, without demanding specialized coding usually needed in FE^2. In the direct FE^2 analysis, both the macroscopic and the microscopic finite element mesh rely on a single model and the micro-macro coupling is carried out by means of linear multi-point constraints (MPCs). Thus, the solution of the equations describing the macro and micro-scale levels are combined into a single analysis. This work aims at employing the direct FE^2 approach to the analysis of elastic-plastic porous materials with cylindrical voids. The results obtained using the direct FE^2 approach are compared with direct numerical simulations (DNS), in which the material heterogeneities are modelled considering a single scale. The comparison allows assessing specific numerical aspects related to the direct FE^2 method, such as its accuracy and the corresponding computational cost. For sake of simplicity, only plane stress problems are addressed.

CONSTITUTIVE FRAMEWORK

The matrix material is assumed to be elastic-plastic and to follow the von Mises flow potential:

$$\Phi = \sigma_e - \sigma_y \tag{1}$$

where σ_y is the material yield stress, which for the sake of simplicity is assumed to be constant. The effective von Mises stress is defined by: $\sigma_e = \sqrt{\frac{3}{2}\boldsymbol{s} : \boldsymbol{s}}$, with $\boldsymbol{s} = \boldsymbol{\sigma} - \sigma_h \mathbf{1}$ and $\sigma_h = \frac{1}{3}\boldsymbol{\sigma} : \mathbf{1}$, being $\mathbf{1}$ the unit second order tensor. Considering an elastic-plastic media, the rate of deformation tensor is assumed to be the sum of an elastic $\boldsymbol{d}^e$ and a plastic part $\boldsymbol{d}^p$:

$$\boldsymbol{d} = \boldsymbol{d}^e + \boldsymbol{d}^p \tag{2}$$

where the elastic part is related to the rate of the stress by the following hypo-elastic law:

$$\overset{\triangledown}{\boldsymbol{\sigma}} = \boldsymbol{C} : \boldsymbol{d}^e = \boldsymbol{C} : (\boldsymbol{d} - \boldsymbol{d}^p) \tag{3}$$

with $\overset{\triangledown}{\boldsymbol{\sigma}}$ being an objective stress rate and $\boldsymbol{C}$ being the isotropic elastic tensor given by:

$$\boldsymbol{C} = \frac{E}{1+\nu}\boldsymbol{I}' + \frac{E}{3(1-2\nu)}\mathbf{1} \otimes \mathbf{1} \tag{4}$$

where E is the Young's modulus, ν is the Poisson's ratio, and $\boldsymbol{I}'$ is the unit deviatoric fourth order tensor. The plastic deformation rate tensor is considered to follow an associated flow rule:

$$\boldsymbol{d}^p = \dot{\lambda}\frac{\partial \Phi}{\partial \boldsymbol{\sigma}} \tag{5}$$

where $\dot{\lambda}$ is a non-negative plastic multiplier satisfying suitable loading/unloading Kuhn-Tucker, $\dot{\lambda} \geq 0$, $\Phi \leq 0$, $\dot{\lambda}\Phi = 0$, and consistency, $\dot{\lambda}\dot{\Phi}$, conditions.

DIRECT FE^2 THEORY

In this section, we briefly outline the main aspects regarding the direct FE^2 theory proposed by Tan et al. (2020). For more details, the reader is referred to the original work. Let us consider a solid body, with its current domain Ω and boundary $\partial\Omega$, under equilibrium conditions. Therefore, the weak formulation can be obtained using the virtual power principle given by:

$$\int_\Omega \boldsymbol{\sigma} : \delta\boldsymbol{d} dV = \int_\Omega \boldsymbol{b} \cdot \delta\boldsymbol{v} dV + \int_{\partial\Omega} \boldsymbol{t} \cdot \delta\boldsymbol{v} dA \tag{6}$$

where $\boldsymbol{\sigma}$ is the Cauchy stress tensor, $\delta\boldsymbol{d} = \frac{1}{2}\left(\nabla\boldsymbol{v} + (\nabla\boldsymbol{v})^T\right)$ is the virtual deformation rate tensor, $\delta\boldsymbol{v}$ is the virtual velocity vector *compatible with all kinematic constraints*, $\boldsymbol{b}$ is the body force vector, and $\boldsymbol{t}$ is the traction vector.

The left-hand side of Eq. (6) is the internal virtual power $\delta W_{int} = \int_\Omega \boldsymbol{\sigma} : \delta\boldsymbol{d} dV$, which is numerically integrated using Gaussian quadrature, such that (considering a macroscopic mesh having n_{el} elements, each one with n_{ip} integration points):

$$\delta W_{int} \approx \sum_{e=1}^{n_{el}} \sum_{\alpha=1}^{n_{ip}} \left(w_\alpha J_\alpha \boldsymbol{\sigma}_\alpha : \delta\boldsymbol{d}_\alpha\right)_e \tag{7}$$

where indices α denotes the integration point in the finite element e, J_α and w_α are the Jacobian and the weight of the respective Gauss point, respectively. In multi-scale analysis, it is assumed that macroscopic quantities (stress and deformation tensors) at each integration point are given by the volume average of the respective microscopic field $\tilde{(\cdot)}$ over a corresponding representative volume element (RVE), with domain $\tilde{\Omega}_\alpha$ and volume $\left|\tilde{\Omega}_\alpha\right|$, such that:

$$\boldsymbol{\sigma}_\alpha = \langle\tilde{\boldsymbol{\sigma}}\rangle_\alpha \quad \text{and} \quad \delta\boldsymbol{d}_\alpha = \left\langle\delta\tilde{\boldsymbol{d}}\right\rangle_\alpha \tag{8}$$

where $\langle\cdot\rangle_\alpha = \frac{1}{|\tilde{\Omega}_\alpha|}\int_{\tilde{\Omega}_\alpha}(\cdot)\,dV$ denotes the volume average over the RVE associated with the integration point α. Therefore, Eq. (7) can be rewritten as:

$$\delta W_{int} \approx \sum_{e=1}^{n_{el}}\sum_{\alpha=1}^{n_{ip}}\left(w_\alpha J_\alpha \left\langle\tilde{\boldsymbol{\sigma}}\right\rangle_\alpha : \left\langle\delta\tilde{\boldsymbol{d}}\right\rangle_\alpha\right)_e \tag{9}$$

which, using the Hill-Mandel lemma, $\left\langle\tilde{\boldsymbol{\sigma}}\right\rangle_\alpha : \left\langle\delta\tilde{\boldsymbol{d}}\right\rangle_\alpha = \left\langle\tilde{\boldsymbol{\sigma}} : \delta\tilde{\boldsymbol{d}}\right\rangle_\alpha$, becomes:

$$\delta W_{int} \approx \sum_{e=1}^{n_{el}}\sum_{\alpha=1}^{n_{ip}}\left(\frac{w_\alpha J_\alpha}{|\tilde{\Omega}_\alpha|}\int_{\tilde{\Omega}_\alpha}\tilde{\boldsymbol{\sigma}} : \delta\tilde{\boldsymbol{d}}dV\right)_e \tag{10}$$

Using Eq. (10) into Eq. (6), we obtain the following weak formulation:

$$\sum_e\sum_\alpha\left(\frac{w_\alpha J_\alpha}{|\tilde{\Omega}_\alpha|}\int_{\tilde{\Omega}_\alpha}\tilde{\boldsymbol{\sigma}} : \delta\tilde{\boldsymbol{d}}dV\right)_e \approx \int_\Omega \boldsymbol{b}\cdot\delta\boldsymbol{v}dV + \int_{\partial\Omega}\boldsymbol{t}\cdot\delta\boldsymbol{v}dA \tag{11}$$

In previous equation, that the right-hand side depends on microscopic quantities, while the left-hand side is entirely given from macroscopic variables. We notice that the total internal virtual power $\delta\tilde{W}_{int}$ coming from all the RVEs, related to the macroscopic integration points, is given by:

$$\delta\tilde{W}_{int} = \sum_{e=1}^{n_{el}}\sum_{\alpha=1}^{n_{ip}}\left(\int_{V_\alpha}\tilde{\boldsymbol{\sigma}} : \delta\tilde{\boldsymbol{d}}dV\right)_e \tag{12}$$

Therefore, in order to comply with the energetic compatibility $\delta W_{int} = \delta\tilde{W}_{int}$, the multiplier outside the integral in Eq. (10) is required to be: $\frac{w_\alpha J_\alpha}{|\tilde{\Omega}_\alpha|} = 1$ (see Eqs. (10) and (12)). Then, reasoning on bidimensional simulations, for a given integration point α of a macroscopic finite element e, the thickness h of the corresponding RVE has to satisfy:

$$h = \frac{J_\alpha w_\alpha}{|\tilde{S}_\alpha|} \tag{13}$$

in which $|S_a|$ stands for the area of the RVE.

Using the finite element method, the macroscopic displacement $\boldsymbol{u}$ (and the virtual velocity $\delta\boldsymbol{v}$) vector is approximated as:

$$\boldsymbol{u} \approx \mathbf{N}\mathbf{u} \tag{14}$$

where $\mathbf{N}$ is a matrix containing the global interpolation functions and $\mathbf{u}$ is the macroscopic nodal displacement vector. In the direct FE^2 method, the finite element method is also used to approximate the microscopic kinematic variables. However, in contrast to standard FE^2, in the direct approach, both the macroscopic and the microscopic finite element mesh are included within the same model (see Fig. 1). The displacements of the microscopic nodes on the RVE boundaries are attached to the nodes of the corresponding macroscopic element. Therefore, the macroscopic displacement vector $\mathbf{u}$ is given from a linear combination in terms of the microscopic counterpart $\tilde{\mathbf{u}}$ (containing the displacements of all RVEs), such that:

$$\boldsymbol{u} \approx \mathbf{N}\mathbf{L}\tilde{\mathbf{u}} \tag{15}$$

in which $\mathbf{L}$ is a matrix containing the constants of the corresponding linear combination. A negligible stiffness is assigned to the macroscopic elements, such that the displacements of the macroscopic mesh depend entirely on the microscopic stiffness arriving from the RVE calculations. Adopting periodic boundary conditions, considering the integration point α of the macroscopic finite element e, the macroscopic and microscopic displacement vectors are related by the following equations (see Tan et al. (2020)):

$$\tilde{\mathbf{u}}_C = \mathbf{N}^e\left(\boldsymbol{x}_\alpha\right)\mathbf{u}^e \tag{16}$$

$$\left(\tilde{\mathbf{u}}_T - \tilde{\mathbf{u}}_B\right)_\alpha = l_\alpha\nabla\mathbf{N}^e\left(\boldsymbol{x}_\alpha\right)\mathbf{u}^e \tag{17}$$

$$(\tilde{\mathbf{u}}_R - \tilde{\mathbf{u}}_L)_\alpha = l_\alpha \nabla \mathbf{N}^e(\boldsymbol{x}_\alpha)\,\mathbf{u}^e \tag{18}$$

where $\boldsymbol{x}_\alpha$ is the position vector of the integration point α, l_α is the size of the corresponding RVE, the subscripts C, T, B, R, and L stand for the centre point, the top, bottom, right and left boundaries of the RVE, respectively (see Fig. 1). Moreover, $\mathbf{N}^e$ is the matrix with the shape functions and $\mathbf{u}^e$ is the displacement vector of the macroscopic element e. In this work, the restrictions arriving from Eqs. (16)-(18) are imposed by means of multi-point constraints (MPCs) using the commercial finite element code ABAQUS/Standard (2019). For details on the implementation, we refer to the works of Tan et al. (2020) and Zhi et al. (2021).

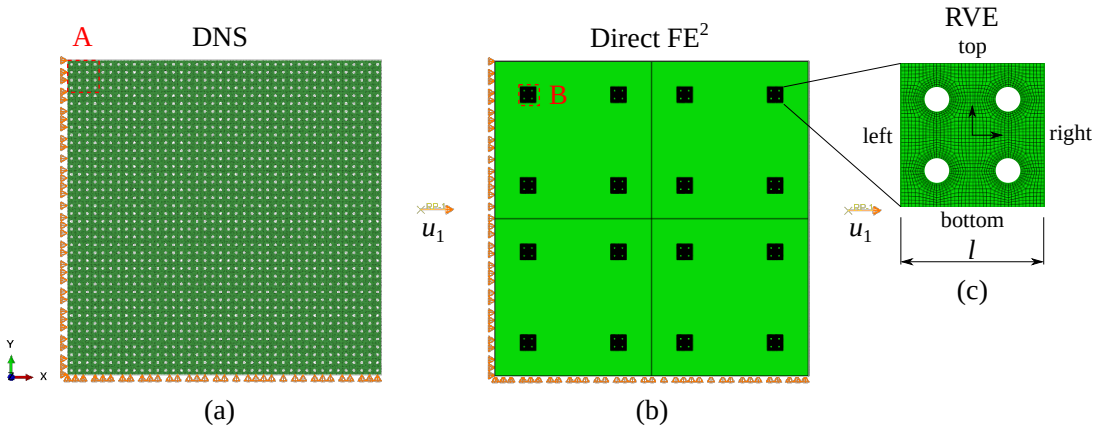

Figure 1 – Finite element mesh used in (a) the direct numerical simulation (DNS) and (b) the direct FE^2 method. (c) Detail of the representative volume element (RVE) mesh.

The simulations consist of a simple tensile test in a squared plate ($1\,\mathrm{mm}\,\mathrm{x}\,1\,\mathrm{mm}$) under plane stress conditions. A perfectly elastic-plastic material is employed, with Young modulus $E = 200\,\mathrm{GPa}$, Poisson ratio $\nu = 0.3$, and a constant yield stress $\sigma_y = 100\,\mathrm{MPa}$. Figure 1 shows the finite element models used in the DNS (Fig. 1(a)) and the direct FE^2 (Fig. 1(b) and (c)) analysis. The DNS has 800,000 CPS4 plane stress elements (ABAQUS/Standard, 2019), while 32,004 CPS4 elements are employed in the direct FE^2 analysis, 4 at the macro-scale and 32,000 at the micro-scale (2,000 in each RVE). The initial RVE-size is set to be $l = 0.05\,\mathrm{mm}$. A total displacement of $u_1 = 0.001\,\mathrm{mm}$ is imposed in the x-direction.

RESULTS

Figure 2 shows the comparison of the force vs. displacement curves for different porosities, $f = 0.05$ and 0.1, employing the direct numerical simulation (DNS) and the direct FE^2 approaches. As it would be expected, increasing the porosity from 0.05 to 0.1, decreased the overall force to impose the total displacement ($u_1 = 0.001\,\mathrm{mm}$), from $\sim 81\,\mathrm{N}$ to $\sim 72\,\mathrm{N}$. The most relevant result shown in Fig. 2 is that the results obtained using the DNS and the direct FE^2 are practically on the top of each other, presenting a difference of $\sim 0.1\%$ for both cases, such that the direct FE^2 is slightly stiffer then the DNS. Based on this observation, the direct FE^2 method can provide very precise results, in comparison with the full simulation, taking much less time, 4% of the CPU time consumed in the DNS analysis.

Figure 3 presents the comparison of the equivalent von Mises stress field for different porosities, $f = 0.05$ and $f = 0.1$, employing the direct numerical simulation (DNS) and the direct FE^2 approaches. The DNS results are shown in Figs. 3(a) and 3(c), considering the region "A" highlighted in Fig. 1(a), while the direct FE^2 results given in Figs. 3(b) and (d) consider the RVE "B" highlighted in Fig. 1(b). From the contour plots displayed in Fig. 3, it is readily seen that both methods provided practically the same von Mises stress fields, with exception of the top region of the DNS plate, where the periodic conditions are not satisfied, given the fact that the top surface is stress free. While the highest value of the equivalent von Mises stress is limited by the constant yield stress ($\sigma_y = 100\,\mathrm{MPa}$), the lowest values are $\sim 21\,\mathrm{MPa}$, for $f = 0.05$, and $\sim 13\,\mathrm{MPa}$, for $f = 0.1$.

CONCLUSIONS

This work consisted of a former study of our group on the multi-scale analysis employing the direct FE^2 method proposed by Tan et al. (2020). Simple numerical simulations based on a uniaxial tensile test were carried out in order to assess specific numerical aspects regarding the corresponding multi-scale approach. Reasoning on the comparison with

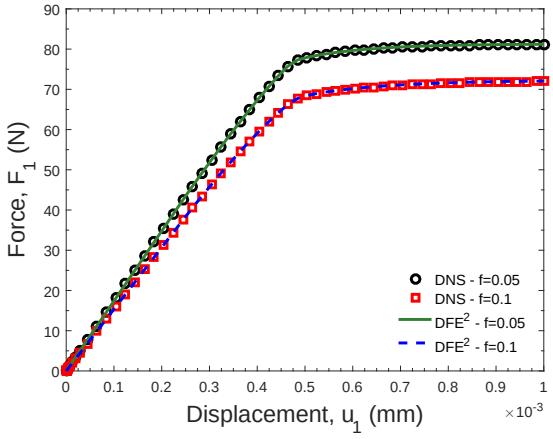

Figure 2 – Comparison of the force-displacement curves for different porosities, $f = 0.05$ and 0.1, employing the direct numerical simulation (DNS) and the direct FE^2 (DFE^2) approaches.

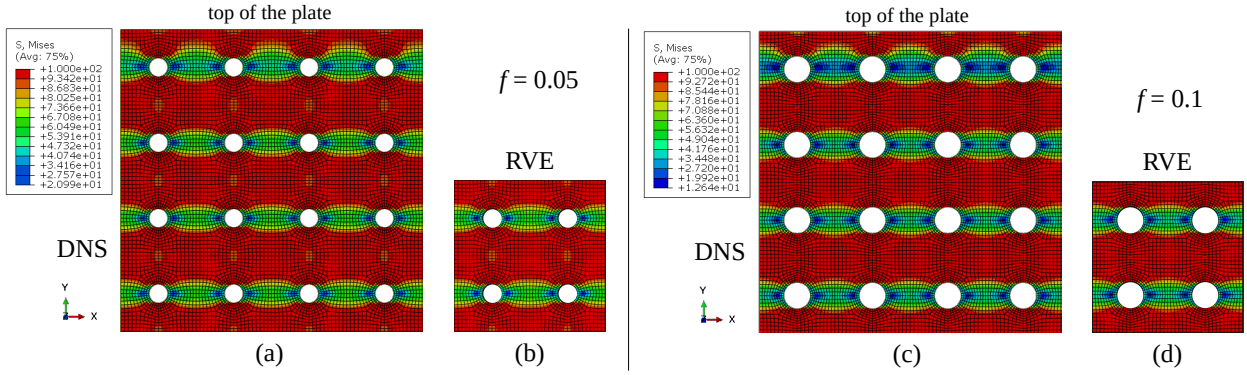

Figure 3 – Comparison of the equivalent von Mises stress field for different porosities, $f = 0.05$, (a) and (b), and $f = 0.1$, (c) and (d), employing the direct numerical simulation (DNS), (a) and (c), and the direct FE^2, (b) and (d), approaches. Figures (a) and (c) show de region "A" highlighted in Fig. 1(a) while figures (b) and (d) show the results considering the RVE "B" highlighted in Fig. 1(b).

direct numerical calculations (DNS), the direct FE^2 approach provided accurate predictions, with differences of $\sim 0.1\%$, taking much less computational time, 4% of the time needed in the DNS calculations. In addition, the direct FE^2 can be easily implemented in commercial finite element codes having multi-point constraint tolls (such as in ABAQUS/Standard (2019)), without demanding the implementation of specific user defined multi-scale material models. Therefore, given the good accuracy of the direct FE^2, its low computational cost and easy implementation, it will be employed in future works of the group dealing with other structural problems with more complex material microstructures and loading conditions.

ACKNOWLEDGMENTS

The author Rodrigo Rossi wishes to acknowledge the support of CNPq, Conselho Nacional de Desenvolvimento Científico e Tecnológico of Brazil, grant number 309430/2021-6, and of FAPERGS, Fundação de Amparo à Pesquisa do Estado do Rio Grande do Sul, grant number 19/2551-0001954-8-1. The author Tiago dos Santos wishes to acknowledge the support of FAPERGS, Fundação de Amparo à Pesquisa do Estado do Rio Grande do Sul, grant agreement 21/2551 - 0000744 - 3.

REFERENCES

ABAQUS/Standard, 2019,. "Simulia, user's manual". Providence, USA: Dassault Systémes. (version 6.19 ed.).
Feyel, F., & Chaboche, J.-L., 2001, "Multi-scale non-linear fe2 analysis of composite structures: damage and fiber size

effects". Revue Européenne des Éléments Finis, Vol. 10, pp. 449–472.
Kouznetsova, V., Brekelmans, W., & Baaijens, F., 2001, "An approach to micro-macro modeling of heterogeneous materials". Computational mechanics, Vol. 27, pp. 37–48.
Matouš, K., Geers, M. G., Kouznetsova, V. G., & Gillman, A., 2017, "A review of predictive nonlinear theories for multiscale modeling of heterogeneous materials". Journal of Computational Physics, Vol. 330, pp. 192–220.
Raju, K., Tay, T.-E., & Tan, V. B. C., 2021, "A review of the fe2 method for composites". Multiscale and Multidisciplinary Modeling, Experiments and Design, Vol. 4, pp. 1–24.
Steinmann, P., & Javili, A., 2016, "Aspects of computational homogenization at finite deformations: A unifying review from reuss' to voigt's bound". Applied Mechanics Reviews, Vol. 68, pp. 22.
Tan, V. B. C., Raju, K., & Lee, H. P., 2020, "Direct fe2 for concurrent multilevel modelling of heterogeneous structures". Computer Methods in Applied Mechanics and Engineering, Vol. 360, pp. 112694.
Yuan, Z., & Fish, J., 2008, "Toward realization of computational homogenization in practice". International Journal for Numerical Methods in Engineering, Vol. 73, pp. 361–380.
Zhi, J., Raju, K., Tay, T.-E., & Tan, V. B. C., 2021, "Multiscale analysis of thermal problems in heterogeneous materials with direct fe2 method". International Journal for Numerical Methods in Engineering, Vol. 122, pp. 7482–7503.

RESPONSIBILITY NOTICE

The authors are the only parties responsible for the printed material included in this paper.